A study of the optical and electronic properties of poly (vinylidene fluoride–trifluoroethylene) copolymer thin films

Y.X. Li [a,b], L. Yan [b], R.P. Shrestha [b], D. Yang [b], Z. Ounaies [c], E.A. Irene [b,*]

[a] *School of Physics and Microelectronics, Shandong University, Jinan, Shandong, 250100, China*
[b] *Department of Chemistry, University of North Carolina, Chapel Hill, NC 27599-3290, USA*
[c] *Department of Aerospace Engineering, Texas A&M University, 3141 TAMU College Station, TX 77843-3141, USA*

Abstract

Thin films of poly(vinylidene fluoride–trifluoroethylene) copolymer were prepared by spin casting from methylethylketone solutions onto SiO$_2$, Si, and quartz slides substrates. The films were optically transparent in the 1.5–4.5 eV (830–280 nm) photon energy range and found to be uniform and smooth as determined using near ultraviolet–visible spectrum and atomic force microscopy, respectively. A Cauchy model was used to fit spectroscopic ellipsometry (SE) data to obtain the refractive index in 1.5–4.5 eV (830–280 nm) that was found to decrease for thinner films. SE performed at several sensitive angles of incidence has revealed slight optical anisotropy for films thicker than 120 nm. Annealing in vacuum densified the films as evidenced by an increase in the refractive index and a decrease in the film thickness. Capacitance versus voltage measurements revealed a static dielectric constant of about 7.5.
© 2006 Elsevier B.V. All rights reserved.

1. Introduction

The copolymer of vinylidene fluoride with trifluoroethylene [P(VDF–TrFE)] has been widely studied for over 35 years since the discovery that this material exhibited piezoelectricity [1] and pyroelectricity [2] in PVDF, and ferroelectricity in P(VDF–TrFE) [3]. These properties led to a broad range of applications [4–7] for this material in electromechanical and microelectromechanical systems, such as ultrasound and audio frequency transducers, sensors, actuators, etc. As a ferroelectric material P(VDF–TrFE) copolymer can be electrically switched between its two stable polarization states, and therefore can be used in high-density nonvolatile random-access memories [8,9]. For nonvolatile memory with a nondestructive readout capability and a smaller cell size, a memory structure based on metal-ferroelectric-semiconductor field-effect transistor has shown promise. Accurate optical properties and film thickness of the P(VDF–TrFE) copolymer as ferroelectric thin films are crucial for the fabrication and un-

derstanding the organic electronic and optical devices and these properties are therefore the focus of this study.

The optical properties of P(VDF–TrFE) copolymer films have been studied both experimentally [10–12] and theoretically [13,14]. Typically the published studies used thick films (>1 μm), and measured film thicknesses using step height methods that are inaccurate for thin organic films. Optical properties have also been determined for thin films of P(VDF–TrFE) copolymer that have been prepared by the Langmuir–Blodgett (LB) method, that yielded highly oriented polycrystalline films with polymer chains parallel to the films and thus with uniaxial anisotropy [10]. At this time no studies have been reported to determine the optical properties of thin P(VDF–TrFE) copolymer films made by the spin casting method that will likely produce films that are less dense and anisotropic.

The present study focuses on the optical properties of P(VDF–TrFE) copolymer that is 50 mol% PVDF and 50 mol% TrFE and that is spin-cast film up to 250 nm film thickness and studied using variable angle spectroscopic ellipsometry (SE) over the photon energy range 1.5–4.5 eV (830–280 nm). The complex dielectric function ($N(\lambda) = n(\lambda) + ik(\lambda)$ where $n(\lambda)$ is the refractive index and $k(\lambda)$ the absorption index) and the film thickness were extracted

* Corresponding author. Tel.: +1 919 966 1652.
  E-mail address: gene_irene@unc.edu (E.A. Irene).

by fitting the experimental data to a parametric model of the sample, and vacuum annealing and optical anisotropy results are also reported. Capacitance versus voltage (C–V) measurements was performed on capacitor structures in order to determine the static dielectric constant K.

2. Experimental procedures

P(VDF–TrFE) copolymer in molar ratio of 50/50 was obtained from Atochem Inc. Solutions of 0.3–4.0 wt.% of the copolymer dissolved in methylethylketone (MEK) were used for spin casting films on quartz slides (Chemglass), single crystal Si and SiO$_2$ (from oxidized Si at 1000 °C in pure O$_2$) substrates using spin speeds from 2000 to 8000 rpm and yielding film thicknesses from about 8.6 to 249.8 nm. The substrates were cleaned using standard RCA procedure [15] prior to deposition and the Si substrate also received an HF dip. Film annealing was done at 120 °C in a vacuum of $\sim 7 \times 10^{-4}$ Pa, in order to investigate the effect of temperature on the optical properties and thickness. Films deposited on quartz slides were used to obtain absorbance near ultraviolet–visible (UV–Vis) spectra using a LAMBDA 950 Spectrophotometer. The film morphology and surface roughness were determined using a Multimode IIIa Atomic Force Microscopy (AFM) and reported in an area of $2 \times 2 \mu m^2$.

The dispersion of the refractive index $n(\lambda)$ and absorption index $k(\lambda)$ and the thickness of copolymer films were obtained by fitting the measured ellipsometric parameters $\Psi(\lambda, \phi)$ and $\Delta(\lambda, \phi)$ to an optical model using J.A. Woollam Inc. analysis software (WVASE32) [16], where $\Psi(\lambda, \phi)$ is the amplitude change between the p-(parallel to the plane of incidence) and s-(perpendicular to the plane of incidence) components of the polarized light that occurs during reflection, and $\Delta(\lambda, \phi)$ is difference in the phase. These measurables were collected in the spectral range 1.5–4.5 eV (830–280 nm) using a custom built variable angle rotating analyzer spectroscopic ellipsometer and a J.A. Woollam Co. model M88 spectroscopic ellipsometer. $\Psi(\lambda, \phi)$ and $\Delta(\lambda, \phi)$ are related to the complex reflection coefficient $\rho(\lambda, \phi)$ and to the ratio of Fresnel coefficients $R_p(\lambda, \phi)$ and $R_s(\lambda, \phi)$ by the formula $\rho(\lambda, \phi) = R_p(\lambda, \phi) / R_s(\lambda, \phi) = \tan(\Psi(\lambda, \phi)) e^{i\Delta(\lambda, \phi)}$ [17].
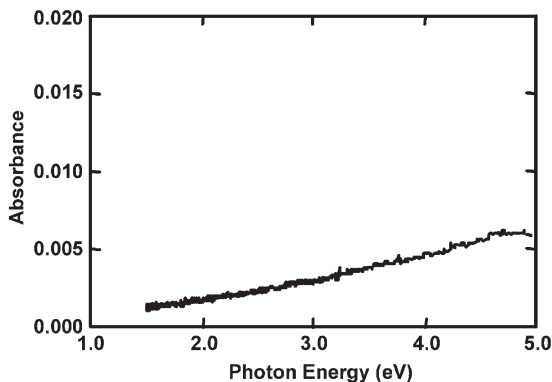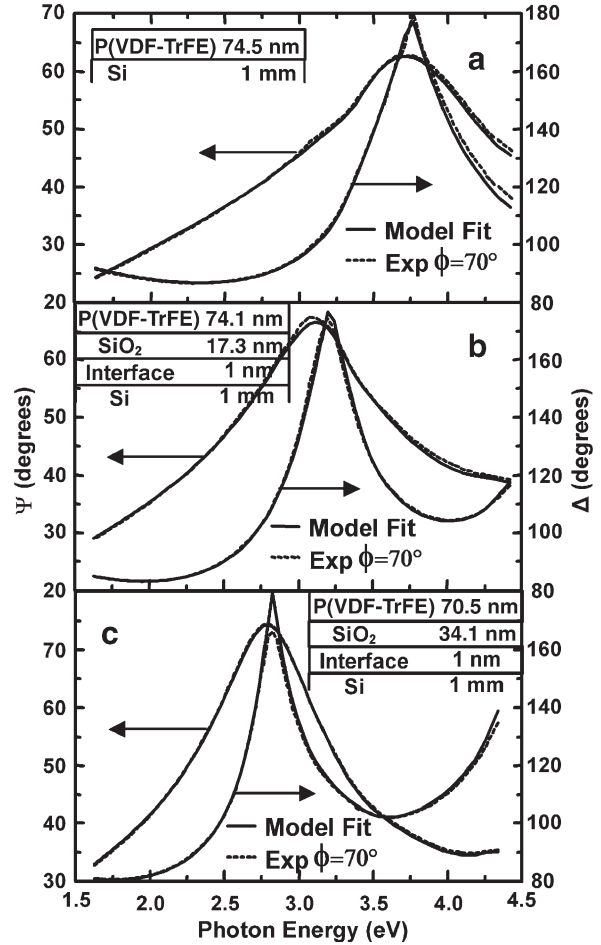

Fig. 2. Ellipsometry measurements of Ψ and Δ (dashed line) from P(VDF–TrFE) films deposited on (a) bare silicon (MSE = 8.9), (b) 17.3 nm SiO$_2$ (MSE = 9.4), and (c) 34.1 nm SiO$_2$ (MSE = 8.5). The insets display the film stack and thickness obtained from the fit.

The Cauchy model was chosen to represent the optical properties of the P(VDF–TrFE) films which are shown below to be optically transparent in the UV–Vis range. The Cauchy formula [17] used is as follows:

$$n(\lambda) = A + \frac{B}{\lambda^2} + \frac{C}{\lambda^4} \qquad (1)$$

Where λ is the wavelength and A, B, and C are parameters that are fit in the analysis. A regression analysis was performed to fit the experimental data to the model. The differences between the model and the experimental data were expressed by the mean-squared error (MSE) which is defined as follows [16]:

$$MSE = \frac{1}{2N-M} \sum_{i=1}^{N} \left[\left(\frac{\Psi_i^{mod} - \Psi_i^{exp}}{\sigma_{\Psi_i}^{exp}} \right)^2 + \left(\frac{\Delta_i^{mod} - \Delta_i^{exp}}{\sigma_{\Delta_i}^{exp}} \right)^2 \right] \qquad (2)$$

Where N is the number of $\Psi(\lambda, \phi)$ and $\Delta(\lambda, \phi)$ pairs used, and M is the number of parameters varied in the regression analysis, while σ is the standard deviation of the experimental data points. The smaller the MSE, the better the agreement of
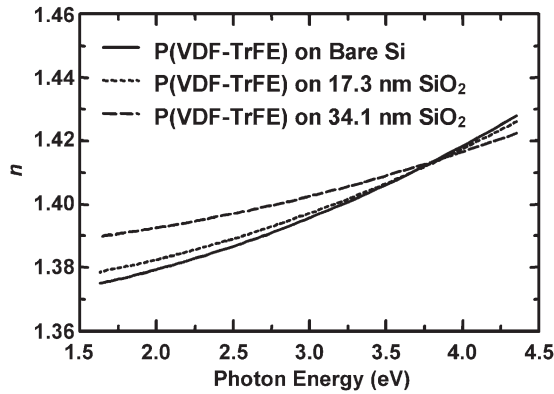

Fig. 1. UV–Vis absorption spectrum of $\sim$20 nm spin cast P(VDF–TrFE) film on a quartz slide substrate.

Fig. 3. The optical refractive indices (n) extracted from SE regression analysis for P(VDF–TrFE) films deposited on bare silicon and silicon dioxide.

Fig. 5. Refractive indices (n) of P(VDF–TrFE) film from Cauchy model with (solid line) and without (dashed line) a BEMA layer for 8.6 nm film.

experimental and model generated results. In order to reduce the correlation among the fitted parameters and improve thickness precision, ellipsometric data were recorded at different angles of incidence ($\phi = 65°$, $70°$, $75°$) in the investigated spectral range and multi sample data analysis was used. In addition, results from independent techniques such as UV–Vis spectroscopy and AFM images were used as input to the models. Optically anisotropy of P(VDF–TrFE) films was checked by rotating
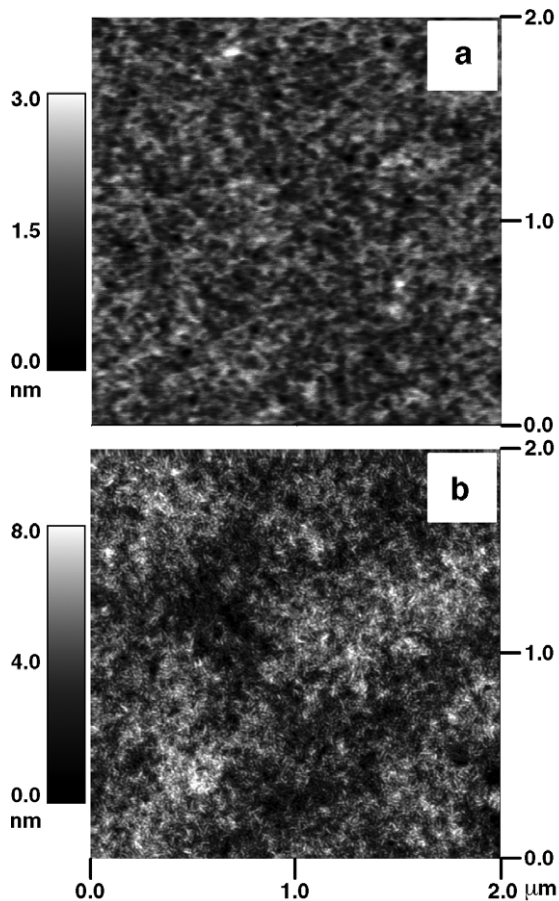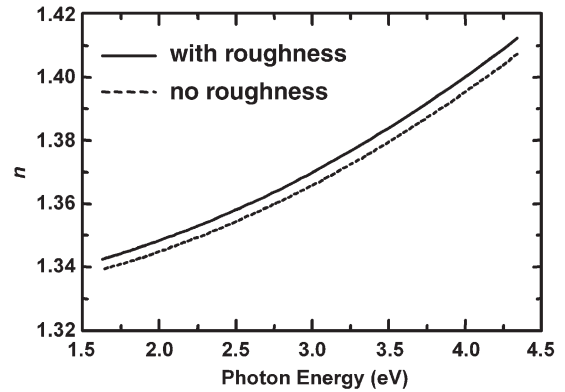
samples in the plane of the substrate to determine in plane anisotropy and at various incident angles to determine out of film plane anisotropy.

Capacitor structures were prepared by evaporating Al through a shadow mask under onto P(VDF–TrFE) films that were deposited onto SiO_2 grown on Si substrates. Capacitance–voltage measurements were performed using a combination HP 4284A LCR meter with a Keithley 236 as the voltage source at high frequency (1 MHz, 20 mV oscillator levels).

3. Results and discussion

3.1. Optical model

Representative UV–Vis spectroscopy results are shown in Fig. 1 for a P(VDF–TrFE) thin film deposited on a quartz slide substrate. It is seen that the P(VDF–TrFE) films display very low absorption in the SE range to be used and can be approximated as being optically transparent in the 1.5–4.5 eV (830–280 nm) range. A Cauchy dispersion formula given above was therefore chosen to represent the optical properties of our P(VDF–TrFE) films.

P(VDF–TrFE) films were deposited on bare silicon and on thin (native oxide < 1 nm) and thick SiO_2 (about 60 nm). The SiO_2 thickness was first determined and then after deposition the P(VDF–TrFE) film thickness and refractive index were
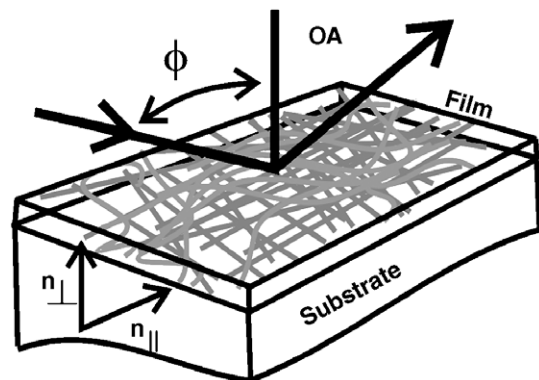

Fig. 4. AFM images of P(VDF–TrFE) films with thickness of (a) 8.6 nm, RMS roughness = 0.4 nm, and (b) 249.8 nm, RMS roughness = 1.3 nm. The scan size is $2 \times 2 \, \mu m^2$.

Fig. 6. Schematic of uniaxial anisotropic polymer thin film: OA is the optic axis, $n_{//}$ and $n_\perp$ are the in plane and out of plane indices, respectively.

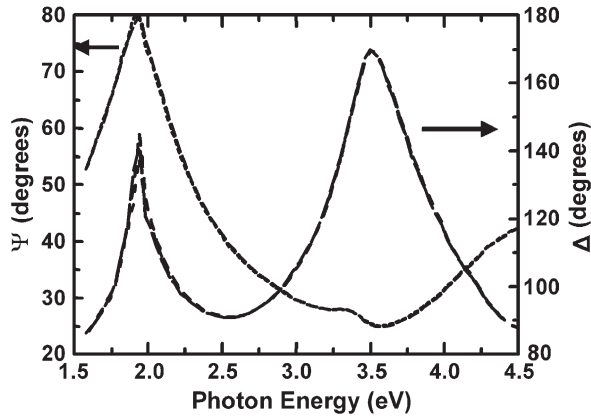Fig. 7. Ψ and Δ taken from 111.5 nm P(VDF–TrFE) film at three different azimuth in-plane angles −0°, 60° and 150°.

determined using a Cauchy model. Typical SE data from three P (VDF–TrFE) samples of about the same thickness (slightly greater than 70 nm) and each on a different substrate are shown in Fig. 2 along with model generated data. The fit is seen to be good with low MSE values (given in the caption of Fig. 2). The refractive indices extracted from the above SE regression analysis are shown in Fig. 3. The observed variation of the index is likely due to the low optical contrast between P(VDF–TrFE) (n about 1.4) and SiO$_2$ (n about 1.5) films and that small errors in the SiO$_2$ thickness will yield larger variation in the extracted P(VDF–TrFE) index and thickness, and this effect is larger for thicker SiO$_2$ films as is seen in Fig. 3. This ellipsometry effect is due to the relative thicknesses of the films in the stack and not to any materials properties.

In order to determine the effects of film roughness on the extracted optical properties AFM was performed. Fig. 4a and b are typical AFM images of P(VDF–TrFE) films with thickness 8.6 nm and 249.8 nm respectively and the root mean squared (RMS) roughness of about 0.4 nm for the 8.6 nm film and 1.3 nm for the 249.8 nm or about 4% and 0.5% of the total thickness of the thin films, respectively. For films thinner than 20 nm, the surface roughness will cause about 0.3 nm decrease in thickness and 0.004 increase in refractive index when the roughness is
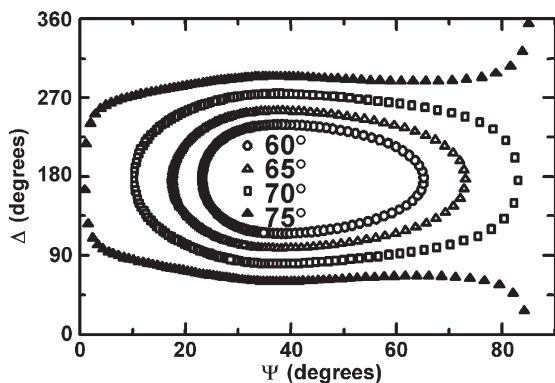

Fig. 9. Ellipsometric Ψ and Δ spectra at different ϕ for 140.7 nm P(VDF–TrFE) film on 53.1 nm SiO$_2$ on Si substrate. Open symbols are the experimental points and continuous lines are fits.

approximated using a Bruggeman effective medium approximation (BEMA) layer (a mixed composition layer with 50% P(VDF–TrFE) and 50% voids and with a thickness of about 1.4× the RMS roughness) on top of the P(VDF–TrFE) layer. But there will be only 0.0009 increase in refractive index and 0.96 nm decrease in thickness by adding the BEMA roughness layer to the optical model for a 249.8 nm thick P(VDF–TrFE) film. Fig. 5 shows the difference between the refractive indices obtained with and without the BEMA layer for a 8.6 nm P(VDF–TrFE) film. It is concluded that the roughness layer does not need to be included in the optical properties determination except for films thinner than 20 nm when the highest accuracy is desired.

3.2. Optical anisotropy

Ellipsomety has recently been used to investigate the optical anisotropy of thin polymer films [18–20]. Fig. 6 (from ref [18])

Fig. 8. Calculated Δ–Ψ trajectories for ϕ from 60° to 75° using an isotropic Cauchy model of P(VDF–TrFE) with film thicknesses 1–320 nm in 2 nm intervals at a photon energy 1.96 eV (632.8 nm, $n=1.40$, $k=0$).
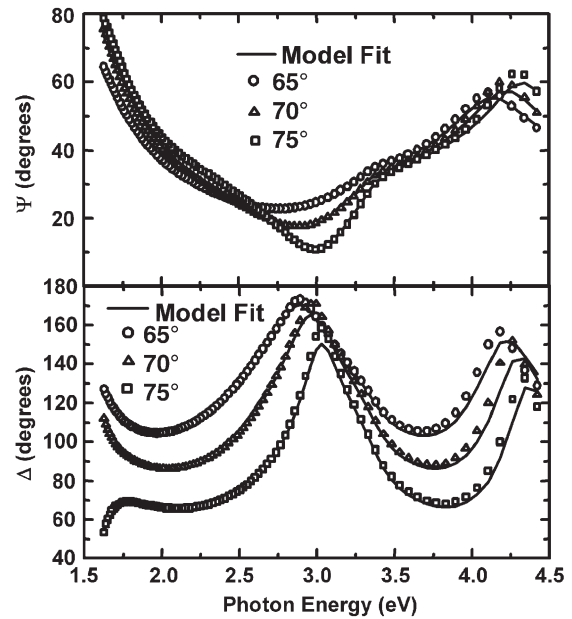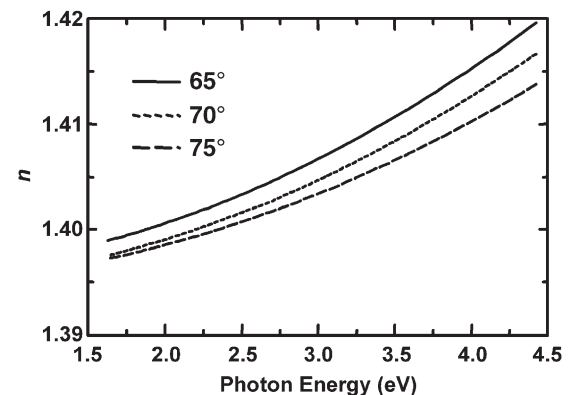

Fig. 10. Refractive indices (n) of 140.7 nm P(VDF–TrFE) film obtained from isotropic Cauchy model fitting at ϕ of 65°, 70° and 75°, respectively.
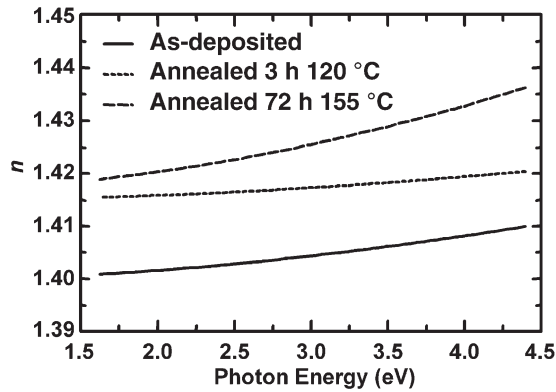
Fig. 11. Refractive indices (*n*) of 127.4 nm P(VDF−TrFE) film as-deposited and annealed 3 h at 120°C and 104 nm P(VDF−TrFE) film annealed 72 h up to 155°C in ∼7×10⁻⁴ Pa vacuum system.

shows that polymer chains that lie in the plane of the film can lead to uniaxial anisotropy, and if the chains are also ordered in the plane of the film biaxial anisotropy results. Out-of-plane uniaxial anisotropy has been reported for LB P(VDF−TrFE) copolymer [10] and other polyfluorene films [21] indicating that the chains lie disordered in the plane of the film.

In-plane anisotropy of spin-cast P(VDF−TrFE) films was investigated using SE at different azimuth angles in-plane −0°, 60° and 150° by rotating the sample in the plane of the film. SE data were obtained on the same spot of the film at incident angle $\phi=70°$. The results shown in Fig. 7 indicate that the three sets of data are almost identical within the error limits indicating that there is no significant in-plane anisotropy in our spin-cast P(VDF−TrFE) films.

In order to determine out of plane anisotropy, SE was performed at multiple angles of incidence (ϕ) from 65° to 75° in 5° intervals. The choice of these angles was made according to the calculated $\Delta–\Psi$ trajectory which is used to evaluate the sensitivity of Ψ and Δ to the incident angle. Fig. 8 showed the calculated $\Delta–\Psi$ trajectories at 1.96 eV (632.8 nm) photon energy with ϕ values from 60° to 75° and with P(VDF−TrFE) thicknesses from 1 to 320 nm at 2 nm intervals. The changes in Δ and Ψ indicate that the most sensitive ϕ values were 65–75° which were therefore selected for use in this study.

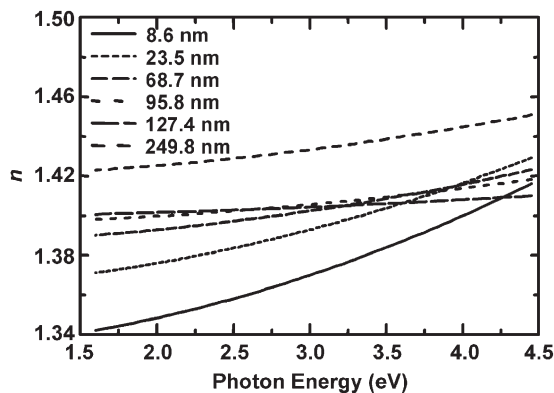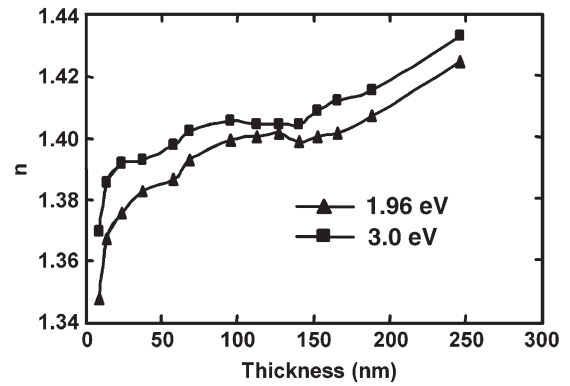Fig. 13. The thickness dependence of the refractive indices (*n*) at 1.96 eV (632.8 nm) and 3.0 eV (415 nm).

Fig. 9 presents the experimental Ψ and Δ values at the ϕ above with Cauchy isotropic fits for 140.7 nm P(VDF−TrFE) film deposited on 53.1 nm SiO₂ on Si substrate. In this case, the MSE was 15.4. However, when a unixial anisotropic fit was used the MSE was lowered to 5.1. The refractive indices *n* extracted from fitting SE data using isotropic model respectively recorded at incident angles ϕ from 65° to 75° are shown in Fig. 10. The difference of *n* at 3.0 eV (415 nm) between 65° and 75° is 0.0033. We did not detect significant out-of-plane anisotropy for films less than 120 nm.

3.3. Annealing studies

It was reported that thermal annealing under vacuum can remove the residual solvent and also improve the crystallinity of P(VDF−TrFE) [22]. Fig. 11 represents the change of refractive index *n* for a 127 nm P(VDF−TrFE) film deposited on 42 nm SiO₂ on Si after annealing for 3 h at 120°C and at ∼7×10⁻⁴ Pa. An increase in *n* of about 0.013 is measured at an incident photon energy of 3.0 eV (415 nm) and a decrease of 2.4 nm (2%) in thickness. Another P(VDF−TrFE) film of similar thickness (104 nm on 41 nm SiO₂) annealed 72 h in vacuum from room temperature to 155°C showed *n* increasing 0.02 and thickness decreasing 3.4 nm (3.3%) and is also displayed in Fig. 11. A comparison of the two samples indicates an initially relatively fast change with annealing but with a longer time to full
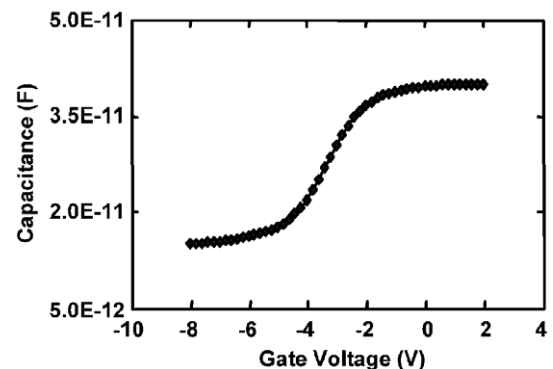

Fig. 12. Refractive indices (*n*) extracted from fitting SE data with different film thicknesses.

Fig. 14. Capacitance versus gate voltage (*C–V*) of 152 nm P(VDF−TrFE)/ 53.9 nm SiO₂/Si sample at 1 MHz.

densification. The small difference in slope between these two samples is due to the P(VDF–TrFE) film thickness difference and will be discussed below.

3.4. Thickness dependence

SE was performed on P(VDF–TrFE) films with different thicknesses. The extracted refractive indices n shown in Fig. 12 indicate that overall n increases with an increase in thickness. In addition, the change with thickness is greater in the thin film regime. This is more easily seen with Fig. 13 that shows the variation of n at $1.96\,eV$ ($632.8\,nm$) and $3.0\,eV$ ($415\,nm$) with thickness. This result may indicate a densification that results in improved crystallinity as was recently reported for thin polystyrene-derived films that showed that the degree of crystallinity depended strongly on the film thickness [23–25].

4. Dielectric constant measurement

The static dielectric constant was measured for Al/P(VDF–TrFE)/SiO$_2$/Si samples of varying thicknesses. Fig. 14 shows a typical $C–V$ curve for a $152\,nm$ P(VDF–TrFE) film on $53.9\,nm$ SiO$_2$ on n-type Si. Based on this ellipsometric thickness, the dielectric constant of P(VDF–TrFE) was calculated to be 7.5 according to the formula $1/C_{tot}=L_{ox}/K_{ox}\varepsilon_0 A+L_p/K_p\varepsilon_0 A$, where C_{tot} is total capacitance, K_{ox}, L_{ox} are the dielectric constant and thickness of SiO$_2$, and K_p, L_p are dielectric constant and thickness of P(VDF–TrFE). Another piece of the same sample was annealed for 3 h in vacuum at $120\,°C$ and a value of 7.4 was obtained indicating that annealing has no significant effect on static dielectric constant. The value of about 7.5 measured for spin cast P(VDF–TrFE) films is lower than the reported value of ~10 for thicker films ($>20\,\mu m$, referred to as bulk material) [26,27].

5. Conclusions

Optical properties of P(VDF–TrFE) films deposited on different substrates were determined using variable angle spectroscopy ellipsometry in $1.5–4.5\,eV$ ($830–280\,nm$) photon energy. A Cauchy model was used to yield a good regression analysis fit. Different substrates do not significantly affect the refractive index which does decrease with thinner films. Variable angles (in plane and out of plane spectroscopic ellipsometry) revealed no in-plane anisotropy, but slight out-of-plane anisotropy for films thicker than $120\,nm$. An increase in refractive index and decrease in thickness were found by annealing films in vacuum. The static dielectric constant K of about 7.5 was measured from $C–V$ measurements.

References

[1] H. Kawai, Jpn. J. Appl. Phys. 8 (1969) 975.
[2] J.G. Bergman Jr., J.H. McFee, G.R. Crane, Appl. Phys. Lett. 18 (1971) 203.
[3] T. Furukawa, M. Date, E. Fukada, Y. Tajistu, A. Chiba, Jpn. J. Appl. Phys. Part 2 19 (1980) L109.
[4] M. Robert, G. Molingou, K. Snook, J. Cannata, K.K. Shung, J. Appl. Phys. 96 (2004) 252.
[5] R. Danz, B. Elling, A. Büchtemann, M. Pinnow, IEEE Trans. Dielectr. Electr. Insul. 11 (2004) 286.
[6] A. Lovinger, J. Sci. 220 (1983) 1115.
[7] T. Furukawa, Phase Transit. 18 (1989) 143.
[8] T.J. Reece, S. Ducharme, A.V. Sorokin, M. Poulsen, Appl. Phys. Lett. 82 (2003) 142.
[9] S.H. Lim, A.C. Rastogi, S.B. Desu, J. Appl. Phys. 96 (2004) 5673.
[10] M. Bai, A.V. Sorokin, D.W. Thompson, M. Poulsen, S. Ducharme, C.M. Herzinger, S. Palto, V.M. Fridkin, S.G. Yudin, V.E. Savchenko, L.K. Gribova, J. Appl. Phys. 95 (2004) 3372.
[11] J.K. Krüger, B. Heydt, C. Fischer, J. Baller, R. Jiménez, K.-P. Bohn, B. Servet, P. Galtier, M. Pavel, B. Ploss, M. Beghi, C. Bottani, Phys. Rev., B 55 (1997) 3497.
[12] Y. Tajitsu, K. Kado, K. Okubo, H. Ohigashi, J. Mater. Sci. Lett. 19 (2000) 295.
[13] M. Cakmak, Y. Wang, J. Appl. Polym. Sci. 37 (1989) 977.
[14] K.S. Spector, R.S. Stein, Macromolecules 24 (1991) 2083.
[15] S. Wolf, R.N. Tauber, Silicon Processing for the VLSI Era, Lattice Press, Sunset Beach, CA, 1990.
[16] J.A. Woollam, Co., Inc. Guide to Using WVASE32®, A Short Course in Ellipsometry, 2001, p. 2.
[17] H.G. Tompkins, W.A. McGahan, Spectroscopic Ellipsometry and Reflectometry: A User's Guide, John Wiley and Sons, INC, 1999.
[18] M. Losurdo, G. Bruno, E.A. Irene, J. Appl. Phys. 94 (2003) 4923.
[19] E.G. Bortchagovsky, Thin Solid Films 307 (1997) 192.
[20] J. Sturm, S. Tasch, A. Niko, G. Leising, E. Toussaere, J. Zyss, T.C. Kowalczyk, K.D. Singer, U. Scherf, J. Huber, Thin Solid Films 298 (1997) 138.
[21] B.P. Lyons, A.P. Monkman, J. Appl. Phys. 96 (2004) 4735.
[22] M.A. Baroque, H. Ohigashi, Polymer 42 (2001) 4981.
[23] C.W. Frank, V. Rao, M.M. Despotopoulou, R.F.W. Pease, W.D. Hinsberg, R.D. Miller, J.F. Rabolt, Science 273 (1996) 912.
[24] F. Xia, B. Razavi, H. Xu, Z.-Y. Cheng, Q.M. Zhang, J. Appl. Phys. 92 (2002) 3111.
[25] Q.M. Zhang, H. Xu, F. Fang, Z.-Y. Cheng, F. Xia, J. Appl. Phys. 89 (2001) 2613.
[26] C. Ang, Z. Yu, L.E. Cross, Appl. Phys. Lett. 83 (2003) 1821.
[27] H. Xu, J. Appl. Polym. Sci. 80 (2001) 2259.